

Numerical simulations of deep penetration problems using the material point method

R. Lorenzo ^{*1}, Renato P. da Cunha ^{2a},
Manoel P. Cordão Neto ^{2b} and John A. Nairn ^{3c}

¹ Department of Civil Engineering, Federal University of Tocantins, Av NS 15 Bala I, Palmas, Tocantins, Brazil

² Department of Civil and Environmental Engineering, University of Brasília,
Campus Darcy Ribeiro, Asa Norte, Brasília, Brazil

³ Wood Science and Engineering, Oregon State University, Corvallis, OR 97331, USA

(Received November 15, 2014, Revised December 31, 2015, Accepted March 17, 2016)

Abstract. Penetration problems in geomechanics are common. Usually the soil is heavily disturbed around the penetrating bodies and large deformations and distortions can occur. The simulation of the installation of displacement piles is a good example of the interest of these types of problems for geomechanics. In this paper the Material Point Method is used to overcome the difficulties associated with the simulations of problems involving large deformation and full displacement type penetration. Recent modifications of the Material Point Method known as Generalized Interpolation Material Point and the Convected Particle Domain Interpolation are also used and evaluated in some of the examples. Herein a footing submitted to large settlements is presented and simulated, together with the processes associated to a driven pile under undrained conditions. The displacements of the soil surrounding the pile are compared with those obtained by the Small Strain Path Method. In addition, the Modified Cam Clay model is implemented in a code of MPM and used to simulate the process of driving a pile in dry sand. Good and rather encouraging agreement is found between compared data.

Keywords: MPM; penetration problems; pile installation effects; large deformation; MCC; SSPM

1. Introduction

In the past years the finite element method (FEM) has become the standard tool for solving a majority of geomechanics problems. Nevertheless, this method, in the Lagrangian description of motion is definitively not suitable to deal with large deformed meshes (Sheng *et al.* 2009). In geomechanics there are typical problems that involve large deformations and distortions, as the penetration of in situ tests (CPT, DMT, SPT), the phenomena of the debris flows, and pile driving (Beuth *et al.* 2007, Di *et al.* 2007, Shin 2009). Numerical modeling of such problems can improve our understanding of the behavior of deep foundations, taking into account somehow their execution methodology, as well as the estimation of soil parameters and safety factors associated

*Corresponding author, Ph.D., E-mail: rlorenzo@uft.edu.br

^a Ph.D., E-mail: rpcunha@unb.br

^b Ph.D., E-mail: porfirio@unb.br

^c Ph.D., E-mail: john.nairn@oregonstate.edu

to a “closer to reality” foundation design.

The analysis of these problems is challenging. The severe mesh distortions that may occur during the process of loading, installation and rupture of a soil structure or, a foundation, have caused the introduction of simplifications to decrease the level of complexity of the simulations. Moreover, the dynamic nature of the considered problems makes the numerical simulations even more challenging (Al-Kafaji 2013).

For the specific case of pile driving, a solution to the soil-structure interaction is also needed. Since the works of Randolph *et al.* (1979), several investigations have been conducted to evaluate and comprehend the influence of the installations effects on the pile’s bearing capacity, and related soil properties to design. Some other studies have also investigated the difference in behavior of different type of piles installed at the same soil. (Dijkstra *et al.* 2011, Grabe *et al.* 2009, Gue 1984, Jardine *et al.* 2013a, Lehane and White 2005, Randolph *et al.* 1979, Yang *et al.* 2006, Zhang and Wang 2009, 2014).

Numerical methods that combine the Lagrangian and Eulerian description of motion have taken place in the simulations of penetrations problems (Sheng *et al.* 2009). Dijkstra *et al.* (2011) used the operator-split method. In this case, the normal Lagrangian calculation is initially performed for the non-advective terms, followed by the calculation of the advective terms. Henke (2010) used FEM and solved the problem of a pile penetration by creating an initial cavity in the place where the pile would be driven. The simplifications introduced by this author forbade the use of the results in the perimeter of the pile. Sheng *et al.* (2009) used the Arbitrary Lagrangian-Eulerian (ALE) method to simulate the process of driving a pile, together with a master-slave technique to simulate the contact between the pile and the soil elements. With the adopted ALE method the simulation was able to effectively “drive” the pile. However, oscillations were observed in the results, tending to amplify when the friction coefficient between the pile and the soil was greater. These authors also tried unsuccessfully to use the Update Lagrangian method, but this simulation of pile driving was aborted due to numerical problems. Zhang and Wang (2014) used the ALE method implemented in the software Abaqus, associated with a simple “breakage” constitutive model, to simulate the penetration of a closed-ended pile within silica sand. This model has indeed achieved good results of the stress distribution inside the sand mass.

The Discrete Element Method (DEM) have also been used to simulate pile installation with good agreements with experimental results (Arroyo *et al.* 2011, Campos *et al.* 2005).

Each of the numerical methods have advantages and disadvantages in the framework of the solid mechanics with large deformations and penetration problems (Shin 2009, Wang *et al.* 2015). Some problems are associated with the properties or characterization of the material as in DEM, other with the large variation of the material stiffness as in FEM.

The MPM has not been extensively used in geomechanics, but it is undoubtedly winning space in problems involving contacts and large deformations. Beuth (2012) used a quasi-static formulation of the MPM to simulate the cone penetration test (CPT). More recently Al-Kafaji (2013) simulates the driven process of closed-ended piles in sands using a complete dynamic formulation of this same method. Nairn and Guilkey (2015) used axisymmetric MPM to simulate deep ballistic penetration of a tungsten rod into steel.

In the present paper the generalized form of the MPM known as “Generalized Interpolation Material Point” (GIMP) (Bardenhagen and Kober 2004) is used. The enhanced interpolations functions introduced to the GIMP method by Sadeghirad *et al.* (2011) and called Converted Particle Domain Interpolation Method (CPDI) was also used. The problem of a shallow foundation loaded to a large settlement level is presented, and the results were scrutinized under distinct

versions of the MPM. The simulation of a pile driven under undrained soil conditions is also carried out, and compared to the method presented by Sagaseta *et al.* (1997) known as “Small Strain Path Method” (SSPM). Finally, the experimental results of Jardine *et al.* (2013b) where small scale piles are driven in dry sand are also simulated.

Given all aforementioned analyses, conclusions could be made on the numerical capabilities of the tested methods to accurately reproduce this type of geotechnical problem.

2. Brief description of the material point method

The MPM is a type of “Particle in Cell method” (Sulsky *et al.* 1995). It combines ideas and procedures of both particle and finite element methods. It has the potential advantages of using the Lagrangian and Eulerian descriptions of kinematics. With the MPM a body is modeled as a group of Lagrangian particles. These particles carry all the information necessary to solve the governing equations. In each time step, the particle variables are interpolated to a fixed mesh in which the equations of motion are solved (Bardenhagen *et al.* 2000). After the solution is obtained, the update solution is extrapolated back to the particles and the state variables and positions are updated. This procedure allows dismissing the computational grid after each step, hence eliminating problems with mesh distortions and tangling (Wieckowski 2004).

The use of different particle characteristic functions defines the variants of the MPM. In the original method, the particle characteristic functions are defined as the Dirac delta function. With this, the particle is represented by a concentrated material point. As this method has problems with particles crossing between cells, the GIMP method was introduced. When the particles are defined with a constant domain, the GIMP method is known as uGIMP. Recently the CPDI method was introduced. In this latter method the particle domain may change its shape and size. This approach avoids some instability problems that appear when the models are submitted to large tractions and potentially handle massive deformations (Sadeghirad *et al.* 2011).

Here a code called NairnMPM is adopted (Nairn 2011). This code was created at Oregon State University. It presents dynamics formulation and has implemented in it a multimaterial contact mode, which introduces some modifications to the contact simulation algorithm presented by Bardenhagen *et al.* (2001) (Lemiale *et al.* 2010). This multimaterial contact allows the establishment of a Coulomb friction law between the bodies. The NairnMPM code has been used with success in several researches before (Bardenhagen *et al.* 2011, Lemiale *et al.* 2010, Nairn 2003, 2006). For most of them, the NairnMPM code was used to problems related to mechanical and wood engineering. Some applications with geotechnical purpose have been conducted too (Llano-Serna 2012, Lorenzo *et al.* 2013). Here the modified Cam Clay model is implemented within the code, being used for some of the examples. The k_0 procedure was also implemented to adapt this code to geotechnical problems, in order to properly generate the initial geostatic stress field.

3. Numerical examples

3.1 Sensitivity analyses of the discretization

A series of two-dimensional analyses were performed for examining the accuracy of the code to different discretization levels. The computing time was also evaluated. The geometry for all th

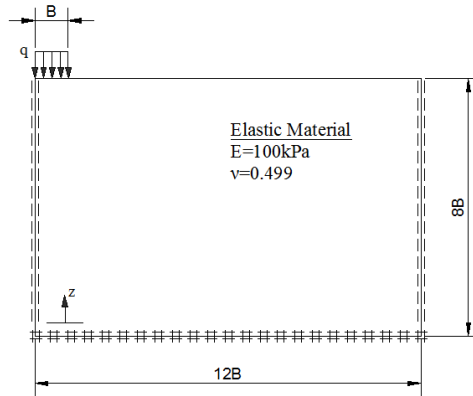


Fig. 1 Strip load on elastic layer

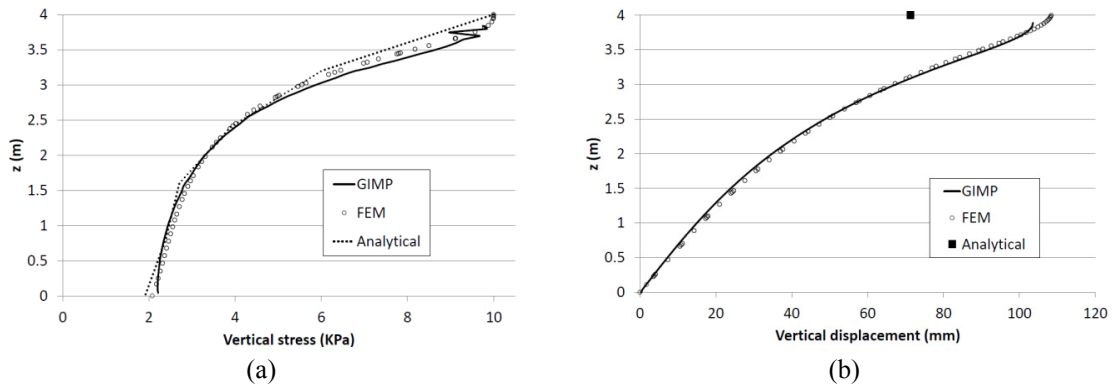


Fig. 2 Vertical stresses and displacement under the center of the footing

models is the same, as presented in Fig. 1. The continuum was assumed to behave as an isotropic linear elastic material. A constant time step computed using the Courant-Friedrichs-Levy condition was used for all the analyses. Poulos and Davis (1974) presented the analytical reference solution for the displacement and stress distribution below the center of the load, considering a rough contact between the layer of material and the rigid base.

The purpose of the simulation was not to represent any real situation, but to define the most efficient discretization level. The parameters were selected just with the aim of comparing the discretization levels.

The analytical solution, as well as the results obtained by both FEM and GIMP methods are presented in Fig. 2. The results using FEM were obtained with Plaxis® program. Table 1 presents the discretization characteristics used in MPM for the 5 tested models that varied cell size and number of particles in each cell. The results presented in Fig. 2 for the GIMP relates to the 50-4 type model. This model is used as the reference for the errors computed in Table 1.

As shown in Fig. 2, the results obtained by FEM and GIMP are almost equal. In the case of displacement the difference between the numerical methods and the analytical solutions is 34%. The analytical solution used herein does not give good results, as has been verified by other authors (Llano-Serna 2012). Fig. 3 depicts the vertical displacement and stresses for all models

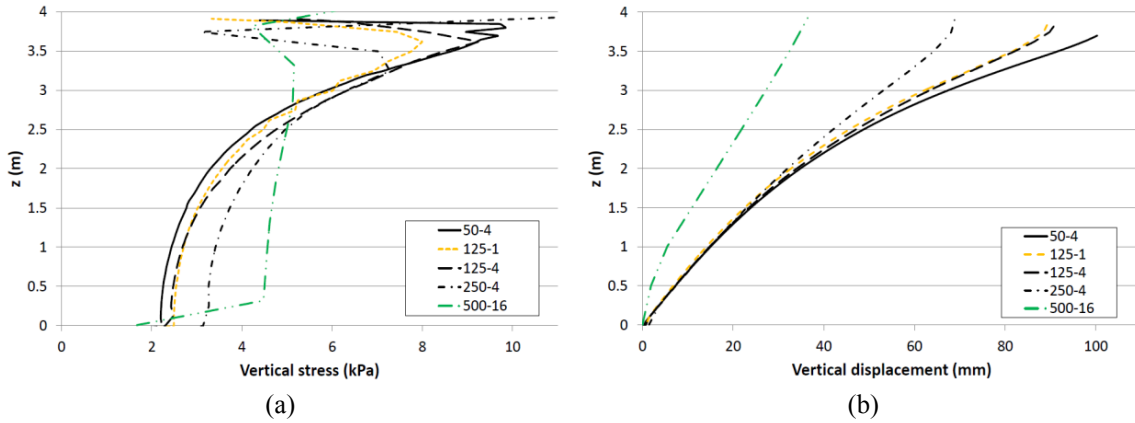


Fig. 3 Vertical stresses and displacement under the center of the footing for the five models

Table 1 ID of the models, discretization and errors between the models

GIMP Model ID	Cell size (mm)	Number of particles per cell	Total of particles	Calculation time (sec)	Average error in vertical stress	Average error in vertical displacement
50-4	50×50	4	38400	119.2	-	-
125-1	125×125	1	1536	10.78	12.48%	4.41%
250-4	250×250	4	1536	4.25	34.90%	12.93%
500-16	500×500	16	1536	1.94	59.97%	32.35%
125-4	125×125	4	6144	35.44	12.44%	3.18%

presented in Table 1.

Table 1 presents the errors among the GIMP models with different discretization levels in relation to the GIMP reference case (50-4). As one notices, the error increases with the increase of the cell dimension, although the total number of particles remains the same. As expected, the calculation time decreases with the increment of the cell size but the error increases faster.

Another feature noticed herein relates to the fact that an increase in the number of particles, using the same cell dimension, does not decrease significantly the error. Hence, unless the geometry of the problem require complex details, it is better to use the smaller number of particles as possible by cell within a robust mesh. This can be understood by doing an analogy with the FEM. The particles in MPM are roughly analogous to Gauss point in the FEM, where the stresses are calculated. Increasing the number of Gauss points does not improve the overall results in FEM analysis, but rather only leads to a better distribution of stresses inside the finite element.

3.2 Rigid footing on soil modeled by the Modified Cam Clay model

A hypothetical test case is simulated to check the applicability of the implemented Modified Cam Clay (MCC) model. In this case, a rigid rough footing loading on top of a horizontal soil surface and submitted to large settlement levels is analyzed. This case is particularly characterized by strong rotations, hence, being ideal for testing the applicability of the numerical methods and the implemented model.

The stress integration scheme for the cases of large deformation is slightly modified with respect to the typical small deformation schemes (Gadala and Wang 2000, Nazem *et al.* 2009). A modification to the Cauchy stress tensor needs to be included. Herein the Jaumann stress rate is used to assure the objectivity of the stress tensor. This means to avoid changes in the stress tensor due to rigid body motions. A method of projecting back the stresses is also included. The projection to the yield surface is done in the direction of the plastic deformations as presented by Potts and Gens (1985). In this way the consistency condition is satisfied considering a tolerance.

Fig. 4 shows the geometry and the properties of the MCC used in the model. Here k_0 is the earth pressure coefficient at rest, γ is the unit weight of the soil, ν is the Poisson's ratio, ϕ is the internal friction angle, λ is the slope of the normal compression line (NCL), κ the slope of the unloading-reloading line and δ is the applied prescribed settlement. The assumed size of the spread footing is equal to $B = 1$ m.

The self-weight is used to generate a non-zero initial stress field. This was introduced by the k_0 procedure as implemented here. A thin layer (0.25 m in thickness) of elastic material is added on

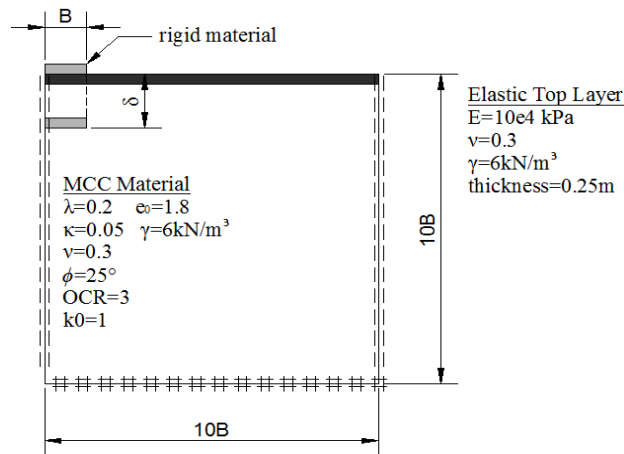


Fig. 4 Rigid footing on soil modeled by MCC model

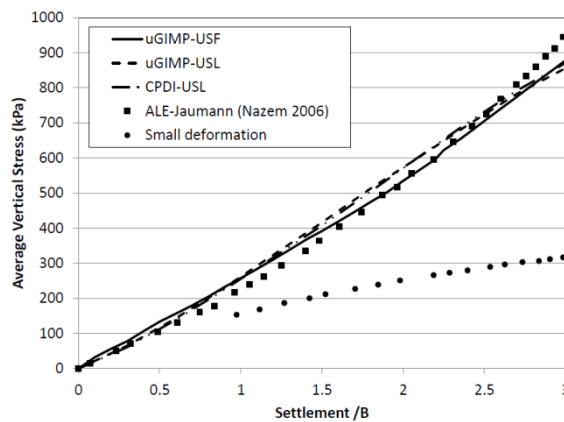


Fig. 5 Rigid footing on soil modeled by MCC model

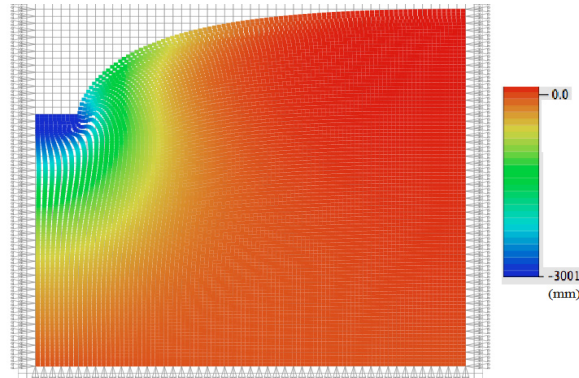


Fig. 6 Deformed shape and vertical displacements (mm) obtained by uGIMP-USF

top of the soil layer, to avoid a slope stability problem when the settlement of the footing gets large, which means a slope failure of the adjacent soil once it becomes highly inclined. The prescribed displacement was applied very slowly to avoid oscillations problems in the model, and because of this no damping was required to preclude this possibility.

For this example, 4 particles per cell were used, for a total of 10100 particles and a structured square uniform mesh with cell size of 200 mm.

This example was documented in Nazem *et al.* (2006) and the results obtained by those authors are used herein as comparison. They used ALE and Update-Lagrange methods for solving the numerical problem. The predicted average vertical pressure under the footing vs. displacement curve is showed in Fig. 5.

The results are presented for the uGIMP and the CPDI method. Both methods are stable until achieving the final prescribed displacement. Also three different moments are used to update the stresses with the uGIMP method. These are namely the update stress first (USF), the update stress last (USL) and update stress average (USAVG). The USAVG approach is not shown because the results are equal to those by the USF method. As it can be seen in Fig. 5, the results obtained by the different variants of the MPM method and the ALE method are very similar. The small deformation case is also included for comparison. The stress update approach USF required less calculation time than the other approaches.

The small differences obtained by the MPM methods and the ALE can be attributed to differences in the interpolations procedures for both methods, and to discrepancies in the defined discretization. In Fig. 6, final deformation level and vertical displacement shade are presented. As can be seen, strong rotations occur in the right side of the foundation.

4. Pile driving in clay

To correctly evaluate the stress levels in the shaft of a driven pile, it is essential to take into account the construction process. As it is known, during the driving sequence the soil close to the pile is heavily distorted (Randolph 2003). The original value of k_0 and the deformation capacity of the soil can therefore change considerably due to that. Hence, the installation processes will affect somehow the behavior of the pile. Some of the first attempts to model the driving stages of piles was done using the Cavity Expansion Method (CEM) (Carter *et al.* 1979). This method however is

limited given the use of a geometric simplification. It solves the problem assuming essentially a cylindrical expansion, which has been shown to be inadequate to simulate the response of the soil near the tip or the top of the piles (Gue 1984). Nevertheless, the analytical solutions obtained by this method are quite useful to rapidly and simply assess the stress level and the displacement field surrounding the pile.

Sagaseta *et al.* (1997) proposed another method that allows predicting the strains in the soil due to a penetration process. This method is known as SSPM and is an extension of the strain path method (SPM) developed by Baligh (1986) for the case of an existing soil free surface. The method assumes that, during a pile driving, the soil moves as an incompressible inviscid fluid around the pile tip. The flow streamlines are used to determine the strain paths of the soil surrounding the pile. This method has been successfully used for the prediction of ground movement by various authors as for example (Lehane and Gill 2004, Sagaseta and Whittle 2001, Xu *et al.* 2006). A numerical procedure is used by Sagaseta *et al.* (1997) to obtain the strain path of the soil in the case of considering large deformations. On the other hand, for small deformations, closed form solutions are given.

Aiming to use the results obtained by the SSPM as a reference, a plain strain analysis of the driving process of a simple wall is done next. Fig. 7 shows the geometry and the properties of the model simulated in MPM. The relation between the length of the simple wall and the semi-thickness is $L/w = 10$. Sagaseta *et al.* (1997) presented the displacements of the soil surrounding a similar wall for the case of considering large deformations with the SSPM. To approximate the results obtained by both methods, a hypothesis similar to the SSPM is adopted for the MPM model, i.e., a von Mises constitutive model was considered for the soil. Furthermore, a low value of the undrained shear strength (C_u) is used. Moreover, the soil near the wall will not have volumetric deformations, since the von Mises model consider that only shear strains occur when the soil reaches a failure stress state. Besides that, $\nu = 0.495$ was initially used and a Coulomb friction coefficient $\mu = 0$ (no friction) was further assumed. These considerations mean that the soil near the wall behaves in a similar way to a fluid.

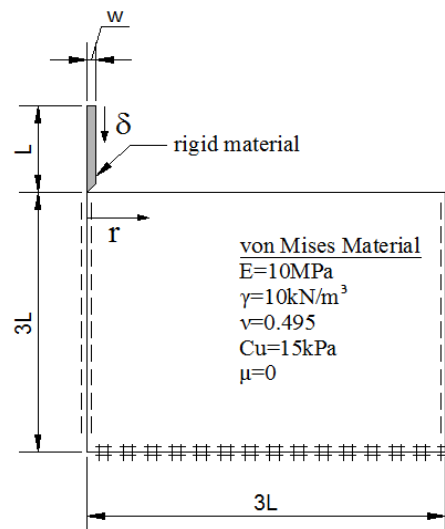


Fig. 7 Geometry and properties of the model for simulation of driving the simple wall

Figs. 8 and 9 respectively show the radial and vertical displacements of the soil when the simple wall has been completely driven. The results were obtained by both GIMP and SSPM methods. The figures show the displacements for three radial distances. Far from the longest adopted distance, no plastic deformations occur and because of that, the model does not represent anymore the hypotheses of the SSPM method and cannot be compared.

Fig. 10 shows the shade of horizontal displacements mobilized during the driving stage of the wall. As it can be seen, a strong heave does occur near the wall.

The results of radial displacements obtained by both methods have a similar trend, and the greatest difference is localized close to the soil's surface. The average error obtained is 18% for $r/w = 1$, 19% for $r/w = 2$ and 13% for $r/w = 3$. In the case of vertical displacements, similar trends have also been noticed, but the derived values are quite different in magnitude. Given that, another model using a value of ν nearest 0.5 was simulated (a value of $\nu = 0.499$ was used, see Fig. 9). The results obtained in this simulation with the new value are closer to those obtained by SSPM, despite the fact that the calculation time increases significantly. However, on the author's opinion the difference between the results may be associated with the fact that the closed form equations proposed by the SSPM were developed under the hypothesis of small strains.

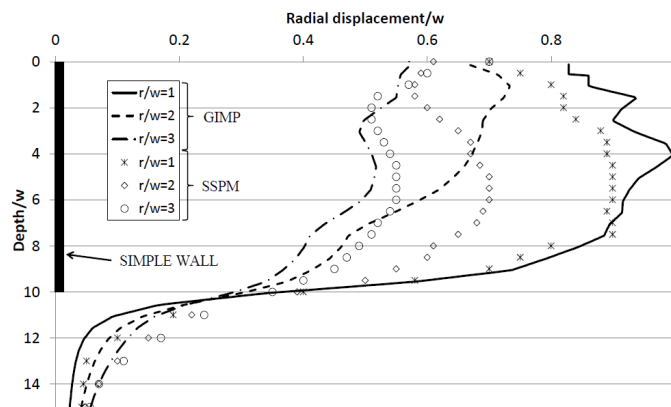


Fig. 8 Radial displacements of the soil after completely driven of the simple wall

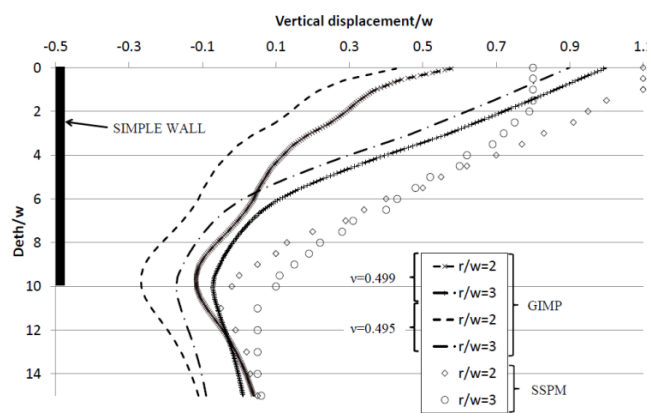


Fig. 9 Vertical displacements of the soil with completely drive of the simple wall

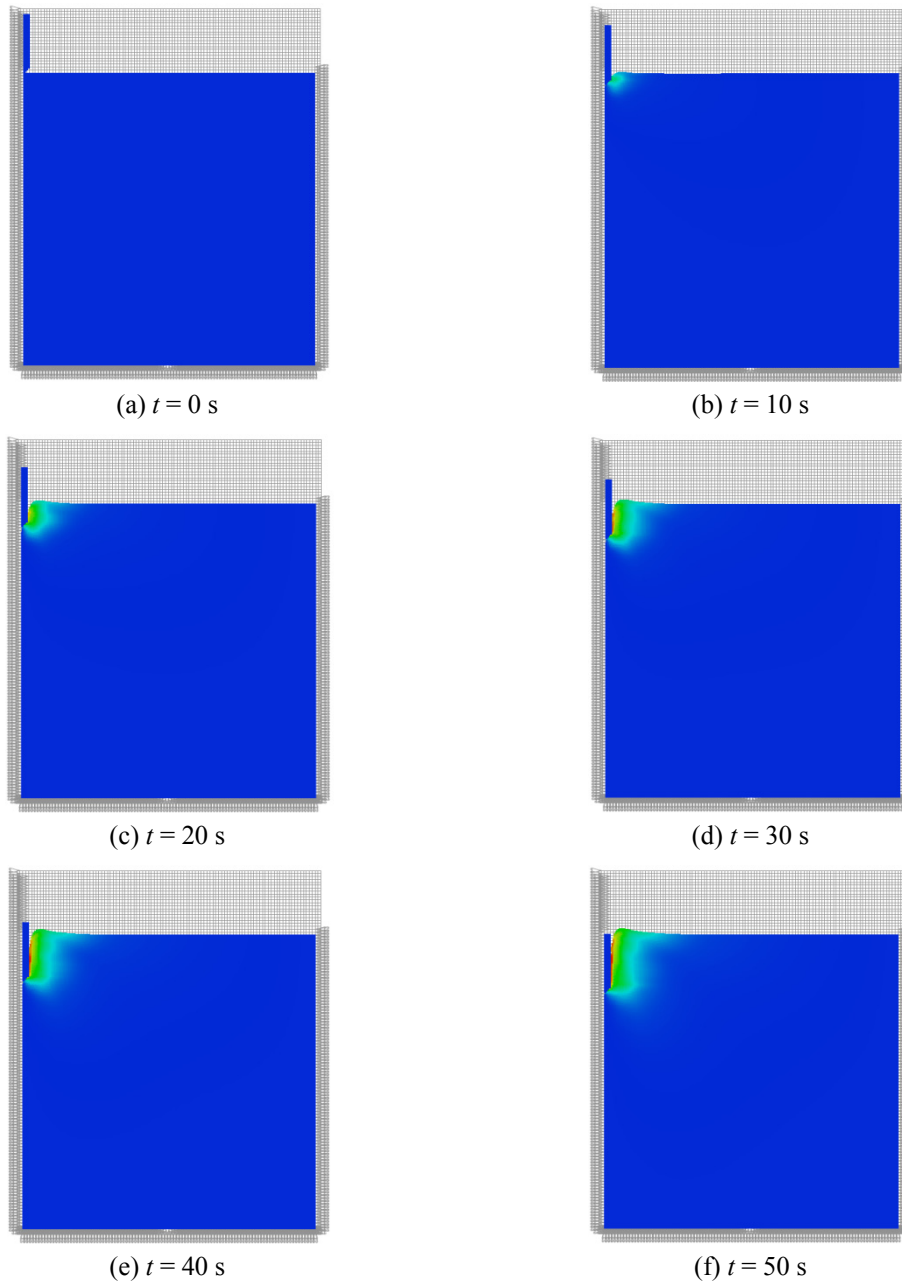


Fig. 10 Horizontal displacement shade during simple wall driving

5. Pile driving in dry sand

The applicability of the MPM code and the implemented model (MCC) to simulate the pile driving in dry sand is considered in this section. For this, the simulation of a (experimental) small scale pile driving phenomena is numerically reproduced. This test was presented in literature by

Jardine *et al.* (2013b).

Fig. 11 shows the dimensions of the calibration chamber and Mini-ICP pile used in the test and the position levels of the sensor inside the mass of soil. Both the chamber and the pile are made of steel and the pile-to-chamber diameter ratio is 33.3. The chamber was filled with Fine NE34 Fontainebleau sand with the index properties given in Table 2. The technique of air pluviation was used to place the sand in the chamber, giving an initial average void ratio of 0.62 to the pluviated deposit. They also reported a $k_0 = 0.45$ and an internal friction angle at critical state between 35.2° and 32.8° with an overconsolidation ratio (OCR) of 1. More details of the complete experiment can be seen in Jardine *et al.* (2013b) and Yang *et al.* (2010). Ring-shear interface tests that reproduce the interface conditions between the pile and the sand showed an average interface friction angle $\delta' = 26^\circ$ (Tsuha *et al.* 2012). This means an interface friction coefficient of $\mu = 0.49$. The values of λ and κ needed to complete the parameters of the MCC model used in the simulation were interpreted from a compression test on the virgin NE34 sand, as presented by (Yang *et al.* 2010), and respectively equivalent to 0.15 and 0.013.

It was simulated herein the test named as Mini-ICP2 by Jardine *et al.* (2013b). In this test, before the driving process, the sand mass was surcharged through a top membrane that had

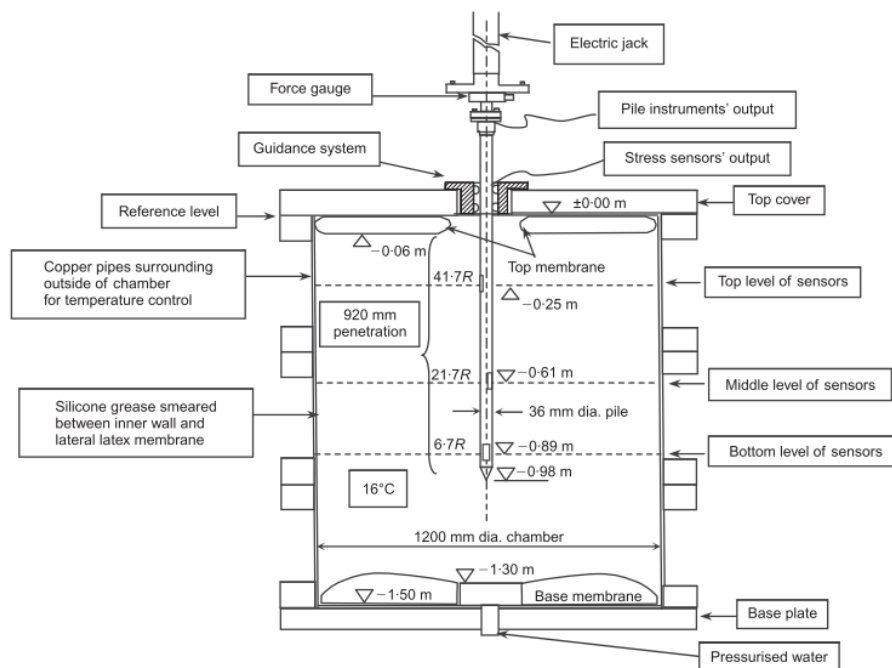


Fig. 11 Schematic diagram of pile driving test showing one example instrument layout (Jardine *et al.* 2013b)

Table 2 Index properties of NE34 Fontainebleau sand (Jardine *et al.* 2013b)

Grain shape	SiO ₂ (%)	Specific gravity	d_{10} (mm)	d_{50} (mm)	d_{60} (mm)	Coefficient of uniformity	e_{max}	e_{min}
Sub-angular	99.70	2.65	0.15	0.21	0.23	1.53	0.90	0.51

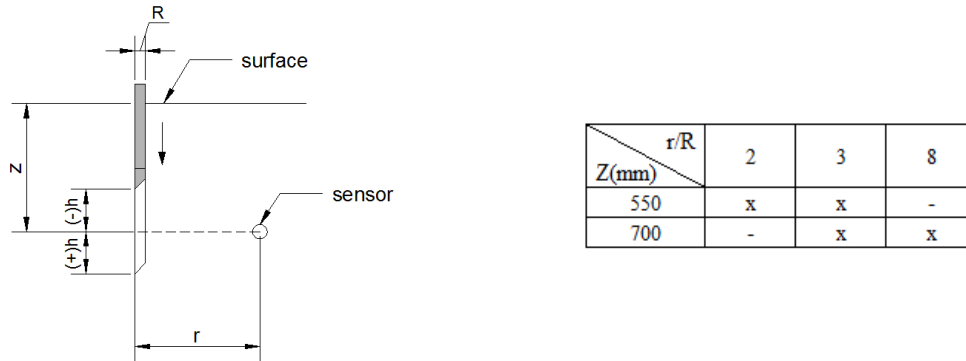


Fig. 12 Schematic diagram of the geometric reference for the results and sensors position

a central internal diameter of 200 mm. A base-pressurized membrane was also used, with a surcharge pressure of 152 kPa, which has generated an initial vertical stress all around the sand deposit of approximately $\sigma_{v0} = 150$ kPa. Mini CPT check tests were carried out before the driving process, reproducing a quasi-constant cone resistance in depth of $q_c = 21 \pm 2$ MPa. The constant jacking rate of the driving process was around 0.5 mm/s. In the numerical simulations, the pile was considered to be a rigid element, thus greatly reducing the computing time. The simulations took into consideration aforementioned sand properties for an OCR of 1.

For the simulation, a first stage is considered in which a surface load of 150kPa is applied. After that the pile is driven.

The stresses inside the sand mass were measured with sensors located at different depth (z) and at certain radial distance from the axis pile (r). Fig. 12 shows a schematic diagram to help in the presentation of the results. The “x” in the chart indicates experimental measurement points.

Fig. 13 shows the GIMP simulated and experimentally measured radial stresses that were generated during the driving process of the pile, both normalized by the measured value of q_c . The stresses were measured at two fixed depth ($z = 550$ mm and 700 mm) and at three distinct radial distances from the pile’s axis ($r/R = 2$, $r/R = 3$ and $r/R = 8$). It can be observed that the values of the vertical axis in the graphs are negative ($h/R < 0$) when the pile tip is above the measuring sensor.

Also clearly noticeable, results from both simulations and experimental data are quite distinct in magnitude, although they maintain a similar trend. The radial stresses slightly reduce or stay constant until the pile’s tip is at $h/R > -20$. Near $h/R = 0$, where the tip of the pile is at the same depth level of the sensor, the radial stress exhibits the maximum value, decrease rapidly afterwards. Hence, from this point on, in the numerical test the stresses decrease until a value close to its initial one, while the experimental results indicate that the radial stress will be at least the double (at the end of the driving process) of its initial value.

Fig. 14 plots similar profiles for the case of the normalized stationary vertical stresses. As in the previous case, experimental and numerical values differ in magnitude. Besides, the model didn’t show the initial decrease of the vertical stresses, with an inflexion point between h/R of -20 to 30. According to Jardine *et al.* (2013a) this behavior suggests axial extension of the soil in the beginning of the driving process – which has not been captured by the numerical model.

These problems, the low values of the horizontal stresses at the end of the driving process and the decrease of the radial stresses at the beginning of the driving process, may be associated with

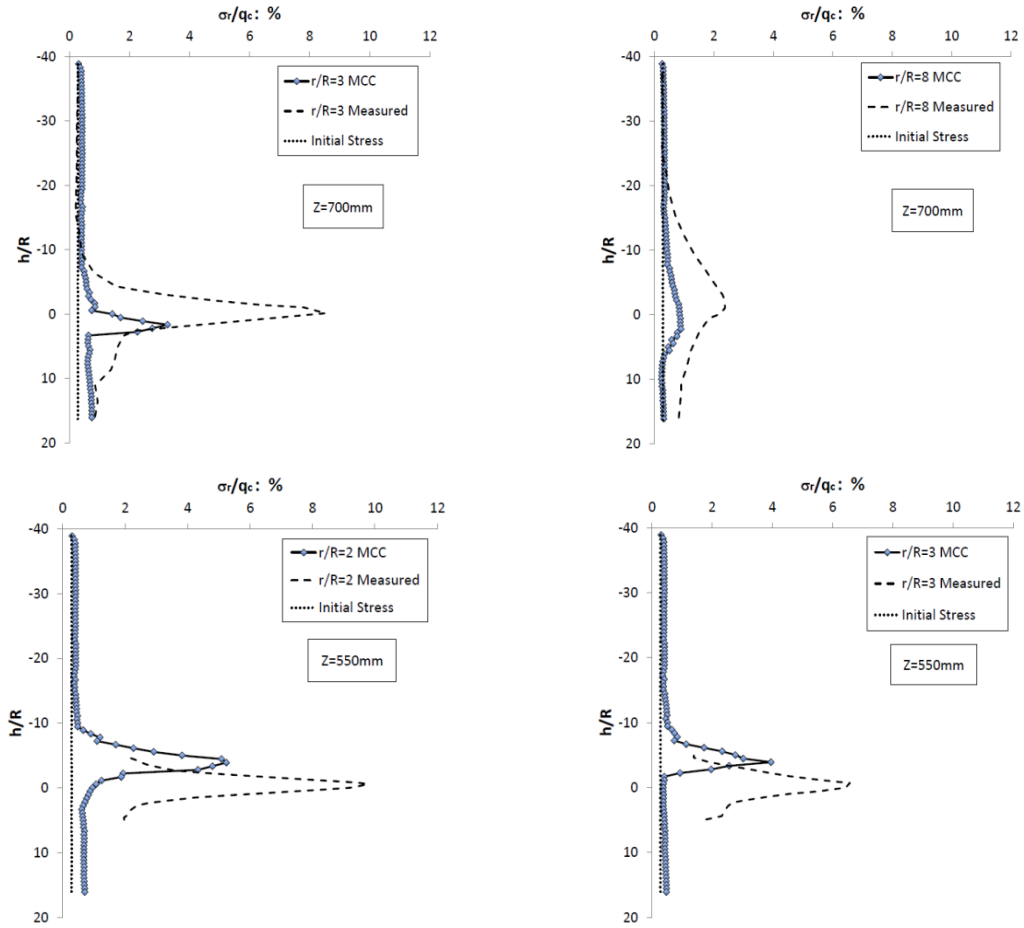


Fig. 13 Normalized stationary radial stress during pile driving

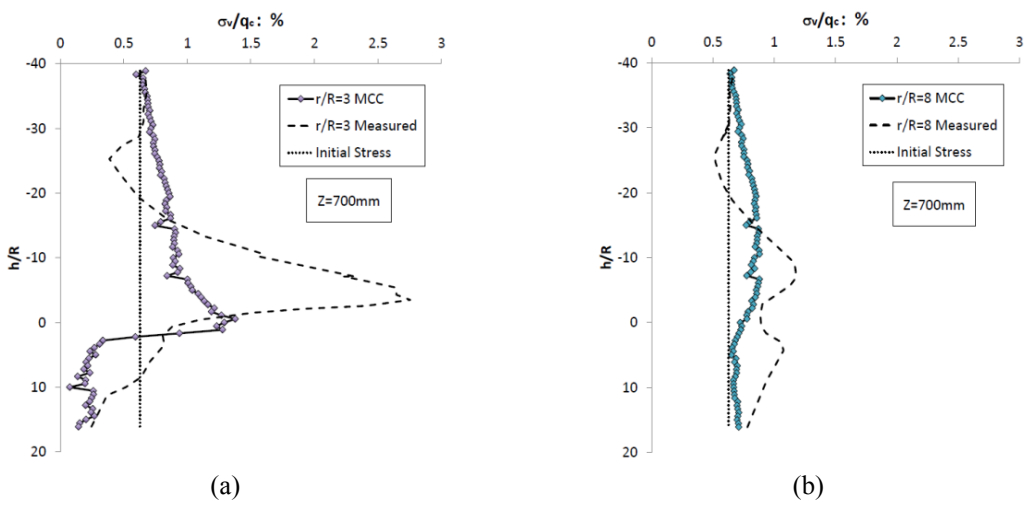


Fig. 14 Normalized stationary vertical stress during pile installation

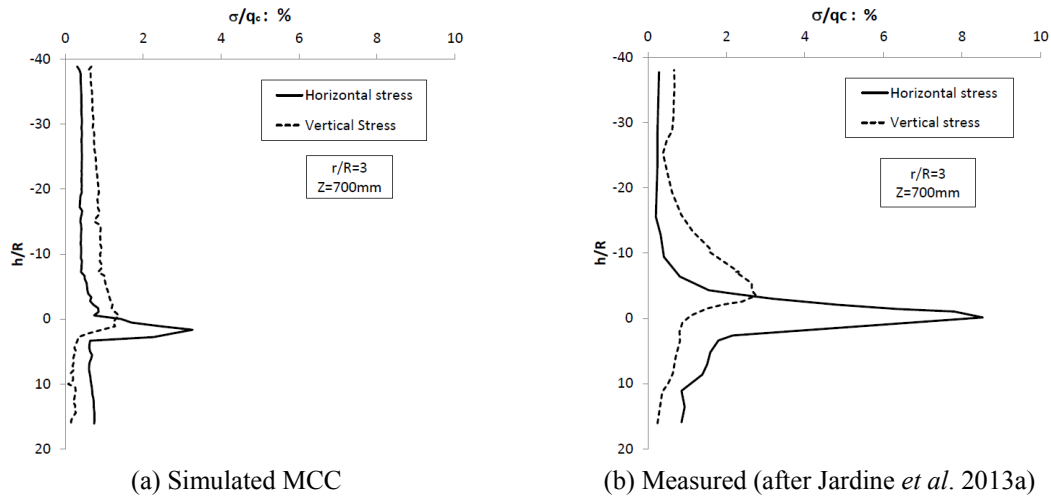


Fig. 15 Horizontal and vertical stress measured and simulated for a specific point during pile installation

the fact that Drucker-Prager rupture criteria estimates the same shearing resistance for extension and compression trajectories.

Fig. 15 presents both, simulated and measured horizontal and vertical stresses along the depth of the tip of the pile, from which the earth pressure coefficient (k) at the sensor depth can be estimated. In the beginning of the penetration the value of k is very close to a $k_0 = 0.45$. At $h/R = -5$ the horizontal stress increases above the vertical one, leading to a $k > 1$. The maximum value of k occurs when the pile tip is at the same depth level of the sensor, decreasing rapidly once the tip passes through it. At the end of the driving process the value of k is greater than 1, characterizing an earth pressure towards the passive value around the pile element.

In general, the experimental values are higher than the numerical ones. In the authors opinion the discrepancies between the results are associated with a phenomenon of soil densification. During the pile penetration the soil is horizontally and vertically displaced. Consequently, a densification of the soil occurs and causes an increasing of the rigidity of the soil. For the same deformation, higher deformations parameters will lead to higher stresses. The densification effect is not considered by the Cam Clay model. For that reason the stresses obtained by the numerical model are lower than the experimental ones.

Fig. 16(a) shows the path of the mean pressure (p') vs. the deviatoric stress (q) for a point inside the sand mass during the pile driving process. As it can be seen, until the pile tip is at (almost the same) depth of the target point ($h/R = 1.7$) the trajectory is similar to a k_0 loading. After that, an unloading path is followed. The change in the loading-unloading path is basically influenced by the change in the direction of the shear stress component τ_{rz} (Fig. 16(b)). When the pile tip passes through the target point the direction of the shear stress component changes, and the magnitude of the radial and vertical stresses also decrease in a fast manner.

This variation of the horizontal and vertical stresses with the installation process highlights the importance of taking these features into account when designing a prefabricated driven pile. Changes in soil density and confining stress levels surrounding the pile will undoubtedly take place, thus changing the pile's final response in terms of its bearing capacity and settlement.

Nowadays such installations effects are “partly” (or empirically in most cases) considered by

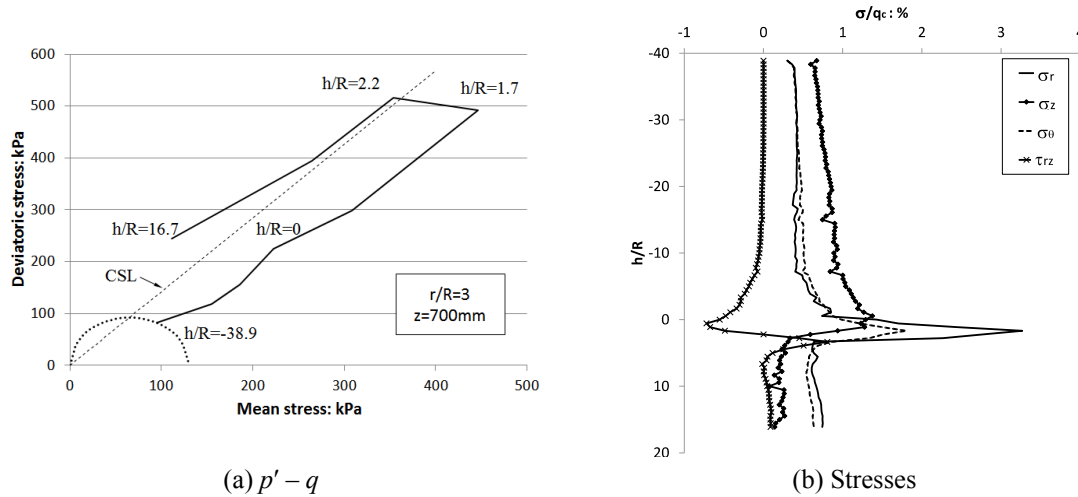


Fig. 16 Stress path during pile drive for the point at $z = 700$ mm and $r/R = 3$

the design methods in foundation engineering. Although it may eventually not represent a bold change in the pile's response, it may be of critical importance in non-classical soils or in complex geotechnical situations, such as non-uniform pile groups, metastable geotechnical materials, or piles subjected to large cyclic loads (as the base of aero-generators). From the existing (empirical) procedures to design allowing for the installation process, the one proposed by Jardine *et al.* (2005) is quite handy when the designers do have access to CPT q_c values in an investigated site. Nevertheless, this in situ testing tool is not yet readily available in many South American countries (or culturally not used for foundation sites, as in Brazil). Besides, this design procedure still lacks a feasible and universal accuracy given its empirical origins.

In other words, research on the installation effects of driven and perhaps bored piles is of utmost importance, and may lead to sharp modifications in today's procedures, at least for some particular cases. Perhaps some advance in this area will come by a specialized (as presented herein) numerical model that can numerically represent the true nature of the mobilized stresses during the pile's execution process. Moreover, Zhang and Wang (2014) point out the importance of considering the breakage mechanism of the sand particles (during driving) to properly account for the stress distribution around the pile. Other intrinsic features of this complex problem can also be incorporated into the constitutive equations, as a more refined rupture criteria or, perhaps, an existing and variable densification process during pile driving.

6. Conclusions

This paper has presented some applications and key points on the use of MPM to the analysis of penetrations problems. Analytical and real problems have been presented and used to validate the implemented MCC model in the NairnMPM code. Based on the presented results, the following conclusions and major observations can be drawn:

- The discretization analyses showed that in order to increase efficiency it is better to use a small number of particles as possible per cell within a robust mesh, rather than using a large

number of particle per cell. More accurate results with a lower computational cost can be obtained in this manner;

- Both uGIMP and CPDI methods were stable until achieving the final prescribed displacement in an example characterized by large deformations and rotations. The results were neither sensitive to the adopted methods nor to the moment when the stresses were updated. Besides, the USF approach to update the stresses required a lower calculation time than the other techniques;
- The displacements caused by the installation of a pile under undrained conditions were evaluated and compared with the SSPM method. The results indicate that the MPM associated with the von Mises material model is well suited to simulate this type of problem. The installation caused a strong heave around the pile, which has been well captured by the numerical simulations;
- The stress distribution obtained by the simulation of a pile driven into a sandy deposit showed a similar trend as the experimental (small scale chamber) values measured by Jardine *et al.* (2013a), although with distinct magnitudes. One could conclude that the present “state” of analysis has potential, besides of indicating the necessity of further improvements to better capture the real phenomena. Perhaps the use of constitutive models that allow for particular features of the behavior of granular soils must be pursued, particularly those features not usually considered by the MCC;
- The ability of the MPM to simulate penetration problems allows evaluation of the behavior of deep foundations with displacement piles in a better way. It considers, for example, the interactions between piles caused by the installations effects in the same group, the equalization process in pile driving in clay an others.
- The results of this paper do show the potential that the presented methodology has to incorporate such important features. The MPM may capture, for instance, the interactions between adjacent piles founded in sand that are caused by successive installation effects in the same group, or the equalization of pore pressures during and after the driving of pile groups in clay.

Acknowledgments

The authors acknowledge the support of the National Brazilian Agency CNPq and the Geotechnical Graduation Program of the University of Brasília for all the related funds that allowed this research.

References

- Al-Kafaji, I.K.J. (2013), “Formulation of a dynamic Material Point Method (MPM) for geotechnical problems”, Ph.D. Thesis; University of Stuttgart, Germany.
- Arroyo, M., Butlanska, J., Gens, A., Calvetti, F. and Jamiolkowski, M. (2011), “Cone penetration tests in a virtual calibration chamber”, *Geotechnique*, **61**(6), 525-531.
- Baligh, M.M. (1986), “Strain path method”, *J. Geotech. Eng.*, **111**(9), 1108-1136.
- Bardenhagen, S.G. and Kober, E.M. (2004), “The generalized interpolation material point method”, *Tech. Sci. Press*, **5**(6), 477-495.
- Bardenhagen, S.G., Brackbill, J.U. and Sulsky, D. (2000), “The material-point method for granular

- materials”, *Comput. Method Appl. Mech. Eng.*, **187**(3-4), 529-541.
- Bardenhagen, S.G., Guilkey, J.E., Roessig, K.M., Brackbill, J.U. and Witzel, W.M. (2001), “An improved contact algorithm for the material point method and application to stress propagation in granular material”, *Comput. Model. Eng. Sci.*, **2**(4), 509-522.
- Bardenhagen, S.G., Nairn, J.A. and Lu, H. (2011), “Simulation of dynamic fracture with the material point method using a mixed j-integral and cohesive law approach”, *Int. J. Fract.*, **170**(1), 49-66.
- Beuth, L. (2012), “Formulation and application of a Quasi-Static material point method”, Ph.D. Thesis; University of Stuttgart, Germany.
- Beuth, L., Benz, T. and Vermeer, P.A. (2007), “Large deformation analysis using a quasi-static material point method”, *Proceedings of the 11th International Conference on Computer Methods in Mechanics*, Łódź-Spała, Poland, June.
- Campos, J.L.E., Vargas, E.A., Bernardes, G., Ibañez, J.P. and Velloso, R.Q. (2005), “Numerical experiments with discrete elements to simulate pile penetration in granular soils”, *Proceedings of CCVI Iberian Latin-American Congress on Computational Methods in Engineering-CILANCE*, Espirito Santo, Brazil, July.
- Carter, J.P., Randolph, M.F. and Wroth, C.P. (1979), “Stress and pore pressure changes in clay during and after the expansion of a cylindrical”, *Int. J. Numer. Anal. Methods Geomech.*, **3**, 305-322.
- Di, Y., Yang, J. and Sato, T. (2007), “An operator-split ALE model for large deformation analysis of geomaterials”, *Int. J. Numer. Anal. Methods Geomech.*, **31**(12), 1375-1399.
- Dijkstra, J., Broere, W. and Heeres, O.M. (2011), “Numerical simulation of pile installation”, *Comput Geotech.*, **38**(5), 612-622.
- Gadala, M.S. and Wang, J. (2000), “Computational implementation of stress integration in FE analysis of elasto-plastic large deformation problems”, *Finite Elem. Anal. Design*, **35**(4), 379-396.
- Grabe, J., Henke, S. and Schümann, B. (2009), “Numerical simulation of pile driving in the passive earth pressure zone of excavation support walls”, *Bautechnik*, **86**(S1), 40-45.
- Gue, S.S. (1984), “Ground heave around driven piles in clay”, Ph.D. Thesis; University of Oxford, UK.
- Henke, S. (2010), “Influence of pile installation on adjacent structures”, *Int. J. Numer. Anal. Method. Geomech.*, **34**(11), 1191-1210.
- Jardine, R.J., Chow, F., Overy, R. and Standing, J. (2005), *ICP Design Methods for Driven Piles in Sands and Clays*, Thomas Telford Publishing, London, UK.
- Jardine, R.J., Zhu, B.T., Foray, P.Y. and Yang, Z.X. (2013a), “Interpretation of stress measurements made around closed-ended displacement piles in sand”, *Géotechnique*, **63**(8), 613-627.
- Jardine, R.J., Zhu, B.T., Foray, P.Y. and Yang, Z.X. (2013b), “Measurement of stresses around closed-ended displacement piles in sand”, *Géotechnique*, **63**(8), 1-17.
- Lehane, B.M. and Gill, D.R. (2004), “Displacement fields induced by penetrometer installation in an artificial soil”, *Int. J. Phy. Modelling Geotech.*, **4**(1), 25-36.
- Lehane, B.M. and White, D.J. (2005), “Lateral stress changes and shaft friction for model displacement piles in sand”, *Can Geotech J.*, **42**(4), 1039-1052.
- Lemiale, V., Nairn, J.A. and Hurman, A. (2010), “Material point method simulation of equal channel angular pressing involving large plastic strain and contact through sharp corners”, *Tech Sci. Press*, **70**(1), 41-66.
- Llano-Serna, M.A. (2012), “Applications of the Material Point Method (MPM) to geotechnical problems”, M.Sc. Dissertation; University of Brasilia, Brasilia, Brazil.
- Lorenzo, R., Cunha, R.P. and Cordão Neto, M.P. (2013), “Material point method for geotechnical problems involving large deformation”, *Proceedings of III International Conference in Particles-Based Methods*, Stuttgart, Germany, September.
- Nairn, J.A. (2003), “Material point method calculations with explicit cracks”, *Comput. Model. Eng. Sci.*, **4**(6), 649-663.
- Nairn, J.A. (2006), “Numerical simulations of transverse compression and densification in wood”, *Wood Fiber Sci.*, **38**(4), 576-591.
- Nairn, J.A. and Guilkey, E. (2015), “Axisymmetric form of the generalized interpolation material point method”, *Int. J. Numer. Methods Eng.*, **101**(2), 127-147.

- Nazem, M., Sheng, D. and Carter, J.P. (2006), "Stress integration and mesh refinement for large deformation in geomechanics", *Int. J. Numer. Methods Eng.*, **65**(7), 1002-1027.
- Nazem, M., Carter, J.P., Sheng, D. and Sloan, S.W. (2009), "Alternative stress-integration schemes for large-deformation problems of solid mechanics", *Finite Elem. Anal. Design*, **45**(12), 934-943.
- Potts, D.M. and Gens, A. (1985), "A critical assessment of methods of correcting for drift from the yield surface in elasto-plastic finite element analysis", *Int. J. Numer. Anal. Methods Geomech.*, **9**, 149-159.
- Poulos, H.G. and Davis, E.H. (1974), *Elastic Solutions for Soils and Rocks*, John Wiley & Sons, Sydney, Australia.
- Randolph, M.F. (2003), "Science and empiricism in pile foundation design", *Géotechnique*, **53**(10), 847-875.
- Randolph, M.F., Carter, J.P. and Wroth, C.P. (1979), "Driven piles in clay-the effects of installation and subsequent effects consolidation", *Géotechnique*, **29**(4), 361-393.
- Sadeghirad, A., Brannon, R.M. and Burghardt, J. (2011), "A convected particle domain interpolation technique to extend applicability of the material point method for problems involving massive deformations", *Int. J. Numer. Method. Eng.*, **86**(12), 1435-1456.
- Sagaseta, C. and Whittle, A.J. (2001), "Prediction of ground movements due to pile driving in clay", *J. Geotech. and Geoenviron. Eng.*, **127**(1), 55-66.
- Sagaseta, C., Whittle, A.J. and Santagata, M. (1997), "Deformation analysis of shallow penetration", *Int. J. Numer. Anal. Methods Geomech.*, **21**(10), 687-719.
- Sheng, D., Nazem, M. and Carter, J.P. (2009), "Some computational aspects for solving deep penetration problems in geomechanics", *Computat. Mech.*, **44**(4), 549-561.
<http://doi.org/10.1007/s00466-009-0391-6>
- Shin, K.W. (2009), "Numerical simulation of landslides and debris flows using an enhanced material point method", Ph.D. Dissertation; University of Washington, Washington, USA.
- Sulsky, D., Zhou, S.-J. and Schreyer, H.L. (1995), "Application of a particle-in-cell method to solid mechanics", *Comput. Phys. Commun.*, **87**(1-2), 236-252.
- Tsuha, C.H.C., Foray, P.Y., Jardine, R.J., Yang, Z.X., Silva, M. and Rimoy, S. (2012), "Behaviour of displacement piles in sand under cyclic axial loading", *Soil. Found.*, **52**(3), 393-410.
- Wang, D., Bienen, B., Nazem, M., Tian, Y., Zheng, J., Pucker, T. and Randolph, M.F. (2015), "Large deformation finite element analyses in geotechnical engineering", *Comput Geotech.*, **65**, 104-114.
- Wieckowski, Z. (2004), "The material point method in large strain engineering problems", *Comput. Method. Appl. Mech. Eng.*, **193**(34-41), 4417-4438.
- Xu, X., Liu, H. and Lehane, B.M. (2006), "Pipe pile installation effects in soft clay", *Geotech. Eng.*, **159**(4), 285-296.
- Yang, J., Tham, L.G., Lee, P.K.K., Chan, S.T. and Yu, F. (2006), "Behaviour of jacked and driven piles in sandy soil", *Géotechnique*, **56**(4), 245-259.
- Yang, Z.X., Jardine, R.J., Zhu, B.T., Foray, P. and Tsuha, C.H.C. (2010), "Sand grain crushing and interface shearing during displacement pile installation in sand", *Géotechnique*, **60**(6), 469-482.
- Zhang, L.M. and Wang, H. (2009), "Field study of construction effects in jacked and driven steel H-piles", *Géotechnique*, **59**(1), 63-69.
- Zhang, Z. and Wang, Y. (2014), "Examining setup mechanisms of driven piles in sand using laboratory model pile tests", *J. Geotech. Geoenviron. Eng.*, **141**(3), 1-12.